

Impurity-induced thermal crossover in fractional Chern insulators

Ke Huang,¹ Sankar Das Sarma,^{2,3} and Xiao Li^{1,*}

¹*Department of Physics, City University of Hong Kong, Kowloon, Hong Kong SAR, China*

²*Condensed Matter Theory Center and Joint Quantum Institute,
University of Maryland, College Park, Maryland 20742, USA*

³*Kavli Institute for Theoretical Physics, University of California, Santa Barbara, California 93106, USA*
(Dated: September 27, 2024)

The recent experimental observation of fractional quantum anomalous Hall (FQAH) states in rhombohedral multilayer graphene has attracted significant attention. One of the most intriguing observations is that the FQAH states at various fractional fillings give way to IQAH states as the temperature is lowered. In this work, we propose a mechanism for the appearance of FQAH states within a finite temperature range in a toy model. The model consists of a flat Chern band and impurities, and we analyze the effects of impurities on the system's behavior at finite temperatures. We believe that the crossover may arise from the competition between the energy penalty for thermal excitations and the increase in entropy. We support our theoretical argument with numerical calculations using exact diagonalization. Our results suggest that impurities may play a crucial role in the crossover from the FQAH to IQAH states in rhombohedral pentalayer graphene.

Introduction.— The search for exotic quantum matter with intrinsic topological order has been a central focus in condensed matter physics over the past few decades. One such example is the fractional Chern insulator (FCI), which serves as an analog of the fractional quantum Hall effect in the absence of any applied magnetic field. Some of the earliest proposals for the FCI were made in the context of a flat Chern band with strong interactions [1–5]. However, the experimental realization of FCI states without an applied magnetic field, now commonly known as the fractional quantum anomalous Hall (FQAH) states, remained elusive until recently. Several research groups have now reported the observation of the FQAH states in various systems, including twisted bilayer MoTe₂ [6–9] and rhombohedral multilayer graphene [10–14]. These groundbreaking experiments have opened new avenues for the study of topological states of matter.

Meanwhile, these experimental breakthroughs have raised new questions regarding the observed FQAH states, especially in rhombohedral pentalayer graphene (PLG). A particularly puzzling finding, as reported recently by Lu et al. [13], is that the FQAH states at some fractional fillings cross over to integer quantum anomalous Hall (IQAH) states. Such a crossover also depends on the applied displacement field, which can control the band structure as well as the screening of the impurities in the sample. This finding is quite unexpected since the FQAH states are fragile and therefore expected to be stable at extremely low temperatures [15]. Therefore, it has attracted immediate attention in the community [16], although a comprehensive understanding of this unexpected crossover is still lacking.

In this Letter, we attempt to provide a quantitative theory to explain why the FQAH effect could only be stabilized within a finite temperature range, $T_e < T < T_{\text{FCI}}$, where T_{FCI} is the temperature scale associated

with the FCI gap or other low-energy excitations [15]. Above T_{FCI} , various excitations are expected to destroy the FQAH effect. The key new ingredient in our theory is the introduction of a lower temperature scale, $T_e > 0$. We argue that, as the temperature is lowered, carriers can be localized by impurities, reducing the “active” carriers in the topological flat band that can form the FQAH state. At $T < T_e$, the effective filling factor is reduced to a value insufficient to maintain the FQAH state, and thus destroying the FQAH effect. As long as $T_e < T_{\text{FCI}}$, the mechanism proposed by our theory could occur in the experiment. Our arguments will be supported by explicit numerical calculations using a toy model with impurities.

In the remainder of this Letter, we first present the toy model and our theoretical argument for the thermal crossover. In particular, we will carefully define the temperature scales T_e and T_{FCI} and explain the mechanism for the crossover. We then support our theory with explicit numerical calculations. We finally conclude with a discussion of the implications of our theory for the experimental situations.

Toy model with impurities.— The essential ingredients of our toy model include a flat Chern band and impurities, as sketched in Fig. 1(a). We start by considering a toy model featuring a well-isolated and flat Chern band that is fractionally filled. We then assume that the whole system can be projected to this flat band and that the band dispersion can be ignored. This assumption is valid when all other energy scales, including interaction, impurities, and temperature, are significantly larger than the width of the flat band but substantially smaller than the gaps between the flat band and the other bands. Consequently, the complete model Hamiltonian reads as

$$H = P_{\text{flat}} V_{\text{int}} P_{\text{flat}} - V_{\text{imp}} \sum_{i=1}^{N_{\text{imp}}} f_i^\dagger f_i, \quad (1)$$

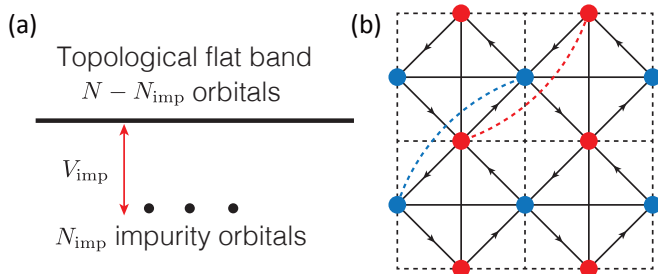


FIG. 1. (a) Illustration of the toy model with impurities. Here, the total system size is N , and N_{imp} impurity orbitals are energetically separated from the topological flat band. (b) Schematic for the single-particle model on a checkboard lattice. The arrows represent the NN hopping, the solid and dashed black lines represent the NNN hopping, and the colored dashed lines represent the NNNN hopping.

where P_{flat} is the projection operator of the flat band, and f_i , serving as the impurities, are the annihilation operators of N_{imp} orthogonal localized single-particle orbitals in the flat band. To simplify the discussion, we model the impurity strength by a single parameter, V_{imp} , instead of considering the most generic case where the impurity orbitals have varying kinetic energies. Nonetheless, we emphasize that the specific choice of the impurities does affect our argument at finite temperatures, which will be discussed in the next section. Finally, the many-body interaction term V_{int} is taken to be the nearest-neighbor interaction, $V_{\text{int}} = U \sum_{\langle i,j \rangle} n_i n_j$. Throughout this work, we will take $U = 1$ as the energy unit of our theory.

For the flat band model, we choose the single-particle model on a checkboard lattice proposed in Ref. [2], which is illustrated in Fig. 1(b). The single-particle Hamiltonian reads as

$$H_{\text{flat}} = \sum_{i,j} t_{ij} c_i^\dagger c_j, \quad (2)$$

which contains nearest-neighbor (NN), next-nearest neighbor (NNN), and next-next-nearest-neighbor (NNNN) hoppings on the lattice. In particular, we set $t_{ij} = te^{i\phi}$ for the NN hopping along the direction specified by the arrows in Fig. 1(b), $t_{ij} = t'$ ($t_{ij} = -t'$) for the NNN hopping specified by the solid (dashed) black lines, and $t_{ij} = t''$ for the NNNN hopping specified by the colored dashed lines. We follow the parameters of Ref. [17] and set $t' = \sqrt{2}t'' = t/(2 + \sqrt{2})$ and $\phi = \pi/4$. These parameters ensure that the bottom band becomes very flat with a Chern number of 1. In addition, when the bottom band is at one third filling, the system becomes an FCI at zero temperature [4, 5] upon introducing the NN interaction V_{int} in Eq. (1). Therefore, the projection operators P_{flat} in Eq. (1) will project onto the flat Chern band in H_{flat} . It is important to note that the absolute energy scale of the hopping

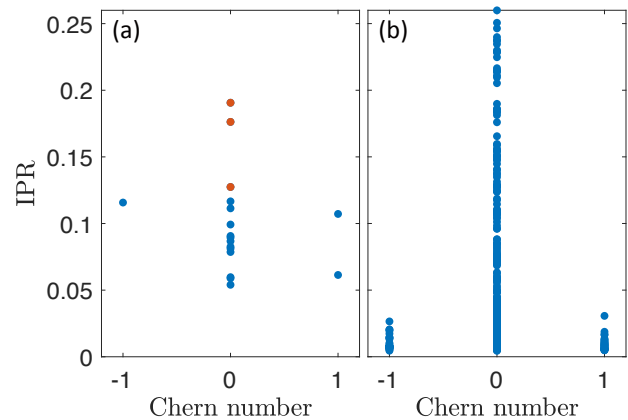


FIG. 2. Chern number and IPR of each orbital in the system of (a) 6×3 unit cells and (b) 20×20 unit cells. Here, the Chern number is calculated by introducing the twisted boundary condition (θ_x, θ_y) , and the horizontal axis is the IPR of the orbitals at $(\theta_x, \theta_y) = (0, 0)$. For (a), we use the same disorder realization as that used in Fig. 3 and Fig. 4. Moreover, the orange dots denote the ones we chose as the $N_{\text{imp}} = 3$ impurity orbitals in the calculation.

terms is irrelevant to Eq. (1) in the flat-band limit.

To create localized orbitals in the Chern band, we follow the method introduced by Zhu et al. [18]. First, we introduce random disorders to the lattice, $V_{\text{dis}} = \sum_j h_j n_j$, where h_j is uniformly distributed in the range $[-1, 1]$. Next, we project this disorder potential onto the flat band using the projection operator P_{flat} , resulting in a new Hamiltonian $P_{\text{flat}} V_{\text{dis}} P_{\text{flat}}$. By diagonalizing this Hamiltonian, we obtain a set of eigenstates that are localized due to the presence of disorder. It is important to note that this random potential is only used to generate the localized orbitals and is not included in the final Hamiltonian. Additionally, not all eigenstates can be localized because the Chern band is topologically nontrivial.

Having generated the localized orbitals, we choose the N_{imp} number of most localized states as the impurity orbitals f_i . To identify such orbitals, we calculate the inverse participation ratio (IPR) and Chern number of each orbital. The IPR of an eigenstate is defined as $I = \sum_j |\psi_j|^4$, where ψ_j is the wavefunction on site j . It approaches 1 (0) for a localized (extended) state, respectively. The Chern number (in the presence of disorder) can be calculated by introducing the twisted boundary condition [19]. Specifically, we require that the wavefunction satisfies $|\psi_{i+N_x, j}\rangle = e^{i\theta_x} |\psi_{i, j}\rangle$ and $|\psi_{i, j+N_y}\rangle = e^{i\theta_y} |\psi_{i, j}\rangle$, where N_x and N_y are the system sizes in the x and y directions, respectively. We then uniformly sample $N_{\theta_x} \times N_{\theta_y}$ values of (θ_x, θ_y) in the range $[0, 2\pi) \times [0, 2\pi)$ and calculate the Chern number of each orbital. Examples of the IPR and Chern number of each orbital in our model are shown in Fig. 2. One crucial observation is that, the localized orbitals do not

contribute to the Hall conductivity because they all have zero Chern number. This is consistent with the fact that they are insensitive to the boundary condition. Such a feature is clearly shown in Fig. 2, especially in a large system. We can now choose the N_{imp} states with the largest IPR and Chern number 0 as the impurity orbitals f_i in our toy model in Eq. (1). Such orbitals are shown as orange dots in Fig. 2(a).

Mechanism for the crossover.— We now explain the mechanism for the crossover from the Fermi liquid (FL) to the FCI state at finite temperatures. Specifically, we consider the filling factor of the system to be around $1/3$. If we denote the system size as N and the particle number as n_e , then $n_e \lesssim N/3$. At zero temperature and in the absence of impurities, this model is known to be an FCI at $1/3$ filling [4, 5]. However, introducing impurities can cause a transition from an FCI to a metallic state [17]. This transition occurs because some particles become trapped in impurity orbitals, reducing the number of “active” particles in the flat band that can form the FCI state. For a strong impurity potential, the number of active particles in the flat band at zero temperature is $n_e - N_{\text{imp}}$. While an FCI state is still stable when the filling factor slightly deviates from $1/3$, if there are too many impurities, $n_e - N_{\text{imp}}$ may fall below the threshold needed to maintain the FCI state. The situation changes at finite temperatures, however. Now thermal excitations from the impurity orbitals to the flat band are possible if they lower the system’s total free energy. These excited particles can increase the number of active particles in the flat band above the threshold, potentially restoring the FCI state.

The above heuristic argument can be made more precise by evaluating the free energy of the system, which allows us to determine the temperature scale T_e at which the crossover occurs. Let’s consider a scenario where, at a finite temperature $0 < T < T_{\text{FCI}}$, x particles (where $x < N_{\text{imp}}$) are excited from the impurity orbitals to the flat band. Because $n_e - N_{\text{imp}} + x < N/3$, the system contains $N_{\text{qh}}(x)$ quasiholes. These quasiholes constitute a low-energy manifold that is separated from the high-energy states by an energy gap Δ_{FCI} [5], which is closely related to T_{FCI} , although other low-energy excitations may also affect T_{FCI} [15]. The total entropy of the system is approximately given by $\ln \left[\binom{N_{\text{imp}}}{x} N_{\text{qh}}(x) \right]$, where $\binom{N_{\text{imp}}}{x}$ represents the number of ways to excite the particles from the impurity orbitals to the flat band and $N_{\text{qh}}(x)$ represents the ways of forming an FCI state after the excitation. Hence, the free energy of the system is approximated by $F \approx xV_{\text{imp}} - T \ln \left[\binom{N_{\text{imp}}}{x} N_{\text{qh}}(x) \right]$, where the first term is the energy penalty for the thermal excitation. The condition that $F \leq 0$ defines an

excitation temperature scale

$$T_e \sim \frac{xV_{\text{imp}}}{\ln \left[\binom{N_{\text{imp}}}{x} N_{\text{qh}}(x) \right]}. \quad (3)$$

Therefore, a crossover to an FCI state at finite temperatures is possible if $T_e < T_{\text{FCI}}$.

The above free energy argument and the criterion $T_e < T_{\text{FCI}}$ for the crossover is anticipated to be valid even for random impurities. However, it is hard to estimate T_e in the latter case because it is generally impossible to determine the energy penalty and the entropy. The advantage of our toy model is that the T_e can be decreased by either increasing $\binom{N_{\text{imp}}}{x}$ or $N_{\text{qh}}(x)$, so the possibility of the crossover can be theoretically and numerically demonstrated.

Numerical results.— We now numerically test our heuristic argument by calculating the finite-temperature density matrix of the toy model using numerical exact diagonalizations. To better observe the temperature induced crossover from the FL to the FCI phase, we need to suppress T_e as much as possible by increasing either $\binom{N_{\text{imp}}}{x}$ or N_{qh} . However, it is difficult to increase $\binom{N_{\text{imp}}}{x}$ numerically because it necessitates an extremely large system size beyond the current capability of exact diagonalizations. Nonetheless, one can readily increase N_{qh} by choosing a filling factor slightly less than the exact fractional filling.

We use particle entanglement spectrum (PES) to characterize the existence of the FCI states [20]. The PES is defined as the spectrum of $\xi = -\ln(\rho_A)$, where the whole system is partitioned into two subsystems A and B , and $\rho_A = \text{tr}_B \rho$ is the reduced density matrix of the finite-temperature density matrix $\rho = e^{-H/T} / \text{tr}[e^{-H/T}]$ in subsystem A . Here, we set the Boltzmann constant $k_B = 1$ for simplicity. The quasihole excitation of an FCI ground state follows the generalized Pauli exclusion principle [5], whereas an FL ground state only has $\binom{n_e}{n_a}$ excitations, where n_a is the particle number of subsystem A . In Fig. 3, we present our calculations on a system with 6×3 unit cells ($N = 18$), $n_e = 5$ particles, and $N_{\text{imp}} = 3$ impurity orbitals. In the clean limit, we verify that the system does contain a low-energy manifold of 126 states separated by an energy gap $\Delta_{\text{FCI}} = 0.05$ from the other states [Fig. 3(a)]. This FCI energy gap vanishes at $V_{\text{imp}} = 0.06$ [Fig. 3(b)], suggesting a zero-temperature phase transition to a metallic state, consistent with the previous study [17]. The disappearance of the FCI ground state at zero temperature is further validated by the absence of an FCI entanglement gap in the PES, as shown in Fig. 3(c). Instead, we find an entanglement gap with 10 states below it, which is consistent with the excitations of an FL. As the temperature increases, however, the entanglement gap at low-temperature vanishes, giving way to another entanglement gap corresponding to the (1,3)-permissible quasihole excitation [5], which is a

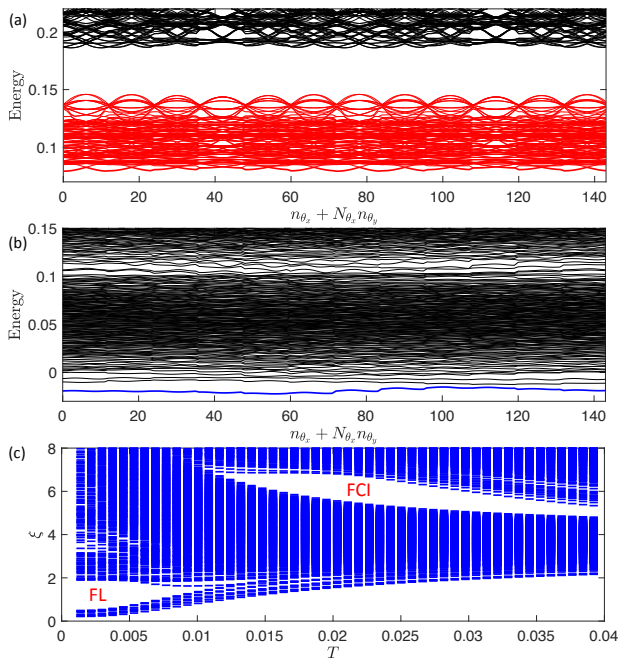


FIG. 3. (a) and (b) are the energy spectrum of the toy model as a function of the flux $n_{\theta_x} + N_{\theta_x} n_{\theta_y}$ for $V_{\text{imp}} = 0$ and $V_{\text{imp}} = 0.06$, respectively. The red lines in (a) highlight the low-energy manifold of the FCI state (the 126 quasi-hole excitations), and the blue line in (b) highlights the ground state of the FL. Here we use $N_{\theta_x} = N_{\theta_y} = 12$. (c) The particle entanglement spectrum (PES) as a function of temperature at $V_{\text{imp}} = 0.06$. For the entanglement gap at $T \lesssim 0.01$, there are 10 states below the gap, in agreement with the quasi-hole excitation of FL. For the entanglement gap at $T \gtrsim 0.01$, there are 330 states below the gap, in agreement with the (1,3)-permissible quasi-hole excitation of FCI [5]. In all plots, the system size is $N_x \times N_y = 6 \times 3$, the particle number is $n_e = 5$, the number of the impurities is $N_{\text{imp}} = 3$, and the PES is obtained by tracing out two particles.

hallmark of an FCI state. From this PES plot, we can infer that while the ground state of the system shown in Fig. 3(b) is metallic at zero temperature, it contains some high-energy FCI-like states. Therefore, as the temperature is raised, the system undergoes a crossover from the FL to the FCI phase. We note that the opening and closing of the entanglement gap at finite temperatures should be regarded as a crossover rather than a genuine phase transition, because the density matrix is a mixed state at finite temperatures. To see this, consider a simplified situation where the total density matrix is a mixture of the ground-state density matrix and the density matrix for the FCI-like states at higher energies,

$$\rho = (1 - \alpha)\rho_{\text{ground}} + \alpha\rho_{\text{FCI}}, \quad 0 \leq \alpha \leq 1. \quad (4)$$

For large α , ρ will exhibit an entanglement gap similar to ρ_{FCI} . However, the presence of an FCI-like entanglement gap in ρ does not necessarily imply $\alpha = 1$. In general, ρ

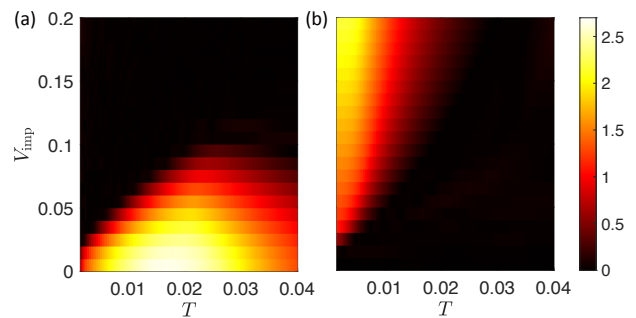


FIG. 4. (a) and (b) are the phase diagram in terms of the entanglement gap for the FCI and FL, respectively. The other parameters are the same as those used in Fig. 3(c).

remains a mixture of the ground state and FCI density matrices. Therefore, observing a finite FCI entanglement gap in ρ suggests that α is large enough for the system to exhibit FCI-like behavior, but does not guarantee a pure FCI state.

In Fig. 4, we present the phase diagram of the FL and FCI entanglement gap to summarize our finding. For $V_{\text{imp}} < 0.1$, we observe a crossover from FL to FCI at finite temperatures. Moreover, the temperature at which the FCI entanglement gap emerges increases with increasing V_{imp} , consistent with our speculation for T_e in Eq. (3). Fig. 4(a) also shows that there is no obvious crossover to the FCI phase for $V_{\text{imp}} > 0.1$, implying that T_e eventually surpasses T_{FCI} for large V_{imp} . Finally, Fig. 4(b) shows the entanglement gap for the FL phase.

Discussion.— Our theory for the thermal crossover is closely related to the experimental observation of the fractional quantum Hall (FQH) state at the $1/7$ filling that appears around $T \approx 100$ mK but disappears for higher or lower temperatures [21]. However, we note that the experimental system is realized on the Landau levels of a two-dimensional electron gas (2DEG), whereas our toy model is defined on a lattice. Moreover, the 2DEG has a long-range Coulomb interaction, whereas our toy model has only NN interactions. We believe that this difference is why the 2DEG tends to form a Wigner crystal at low carrier densities, but the toy model here forms a Fermi liquid. Nonetheless, we emphasize that the nature of the ground state should not affect the validity of our argument, which is based on the competition between the energy penalty and the entropy increase.

It is interesting to discuss the connection of our theory to the recent experiments in the PLG, where a crossover from FQAH phase to IQAH phase is observed for filling factor $\nu > 1/2$ [13]. These experiments correspond to the particle-hole conjugate of our theory ($\nu \rightarrow 1 - \nu$ and $V_{\text{imp}} \rightarrow -V_{\text{imp}}$). In the particle-hole conjugate of our theory, the holes will first occupy the impurity orbitals, which have Chern number zero. Therefore, the ground state will have Chern number one if there are no holes in the topological flat band or the holes in the

flat band are localized by the disorders. As a result, the crossover captured by our theory becomes the one from IQAH to FQAH effect. We also emphasize that the crossover described in our theory needs some fine tuning in the sense that the system must have an appropriate combination of the impurity strength and entropy to make $T_e < T_{\text{FCI}}$ and manifest an obvious crossover. Due to the strong sample-to-sample variations in these factors, we anticipate that this crossover should be experimentally observable in certain samples. However, when T_e is very small, the crossover may occur at a temperature far beyond the current experimental reach. This could explain why the crossover has only been observed for specific ranges of the displacement field, and not in all samples.

Acknowledgement.— K.H. and X.L. are supported by the Research Grants Council of Hong Kong (Grants No. CityU 11300421, CityU 11304823, and C7012-21G) and City University of Hong Kong (Project No. 9610428). K.H. is also supported by the Hong Kong PhD Fellowship Scheme. S.D.S. is supported by the Laboratory for Physical Sciences through the Condensed Matter Theory Center (CMTC) at the University of Maryland. This research was supported in part by grant NSF PHY-2309135 to the Kavli Institute for Theoretical Physics (KITP).

* xiao.li@cityu.edu.hk

- [1] E. Tang, J.-W. Mei, and X.-G. Wen, High-Temperature Fractional Quantum Hall States, *Phys. Rev. Lett.* **106**, 236802 (2011).
- [2] K. Sun, Z. Gu, H. Katsura, and S. Das Sarma, Nearly Flatbands with Nontrivial Topology, *Phys. Rev. Lett.* **106**, 236803 (2011).
- [3] T. Neupert, L. Santos, C. Chamon, and C. Mudry, Fractional Quantum Hall States at Zero Magnetic Field, *Phys. Rev. Lett.* **106**, 236804 (2011).
- [4] D. Sheng, Z.-C. Gu, K. Sun, and L. Sheng, Fractional quantum Hall effect in the absence of Landau levels, *Nat. Commun.* **2**, 389 (2011).
- [5] N. Regnault and B. A. Bernevig, Fractional Chern Insulator, *Phys. Rev. X* **1**, 021014 (2011).
- [6] J. Cai, E. Anderson, C. Wang, X. Zhang, X. Liu, W. Holtzmann, Y. Zhang, F. Fan, T. Taniguchi, K. Watanabe, Y. Ran, T. Cao, L. Fu, D. Xiao, W. Yao, and X. Xu, Signatures of fractional quantum anomalous Hall states in twisted MoTe₂, *Nature* **622**, 63 (2023).
- [7] Y. Zeng, Z. Xia, K. Kang, J. Zhu, P. Knüppel, C. Vaswani, K. Watanabe, T. Taniguchi, K. F. Mak, and J. Shan, Thermodynamic evidence of fractional Chern insulator in moiré MoTe₂, *Nature* **622**, 69 (2023).
- [8] H. Park, J. Cai, E. Anderson, Y. Zhang, J. Zhu, X. Liu, C. Wang, W. Holtzmann, C. Hu, Z. Liu, T. Taniguchi, K. Watanabe, J.-H. Chu, T. Cao, L. Fu, W. Yao, C.-Z. Chang, D. Cobden, D. Xiao, and X. Xu, Observation of fractionally quantized anomalous Hall effect, *Nature* **622**, 74 (2023).
- [9] F. Xu, Z. Sun, T. Jia, C. Liu, C. Xu, C. Li, Y. Gu, K. Watanabe, T. Taniguchi, B. Tong, J. Jia, Z. Shi, S. Jiang, Y. Zhang, X. Liu, and T. Li, Observation of Integer and Fractional Quantum Anomalous Hall Effects in Twisted Bilayer MoTe₂, *Phys. Rev. X* **13**, 031037 (2023).
- [10] Z. Lu, T. Han, Y. Yao, A. P. Reddy, J. Yang, J. Seo, K. Watanabe, T. Taniguchi, L. Fu, and L. Ju, Fractional quantum anomalous Hall effect in multilayer graphene, *Nature* **626**, 759 (2024).
- [11] J. Xie, Z. Huo, X. Lu, Z. Feng, Z. Zhang, W. Wang, Q. Yang, K. Watanabe, T. Taniguchi, K. Liu, Z. Song, X. C. Xie, J. Liu, and X. Lu, Even- and Odd-denominator Fractional Quantum Anomalous Hall Effect in Graphene Moiré Superlattices (2024), arXiv:2405.16944 [cond-mat.mes-hall].
- [12] D. Waters, A. Okounkova, R. Su, B. Zhou, J. Yao, K. Watanabe, T. Taniguchi, X. Xu, Y.-H. Zhang, J. Folk, and M. Yankowitz, Interplay of electronic crystals with integer and fractional Chern insulators in moiré pentalayer graphene (2024), arXiv:2408.10133 [cond-mat.mes-hall].
- [13] Z. Lu, T. Han, Y. Yao, J. Yang, J. Seo, L. Shi, S. Ye, K. Watanabe, T. Taniguchi, and L. Ju, Extended Quantum Anomalous Hall States in Graphene/hBN Moiré Superlattices (2024), arXiv:2408.10203 [cond-mat.mes-hall].
- [14] Y. Choi, Y. Choi, M. Valentini, C. L. Patterson, L. F. W. Holleis, O. I. Sheekey, H. Stoyanov, X. Cheng, T. Taniguchi, K. Watanabe, and A. F. Young, Electric field control of superconductivity and quantized anomalous Hall effects in rhombohedral tetralayer graphene (2024), arXiv:2408.12584 [cond-mat.mes-hall].
- [15] H. Lu, B.-B. Chen, H.-Q. Wu, K. Sun, and Z. Y. Meng, Thermodynamic Response and Neutral Excitations in Integer and Fractional Quantum Anomalous Hall States Emerging from Correlated Flat Bands, *Phys. Rev. Lett.* **132**, 236502 (2024).
- [16] S. Das Sarma and M. Xie, Thermal crossover from a Chern insulator to a fractional Chern insulator in pentalayer graphene (2024), arXiv:2408.10931 [cond-mat.mes-hall].
- [17] S. Yang, K. Sun, and S. Das Sarma, Quantum phases of disordered flatband lattice fractional quantum Hall systems, *Phys. Rev. B* **85**, 205124 (2012).
- [18] Q. Zhu, P. Wu, R. N. Bhatt, and X. Wan, Localization-length exponent in two models of quantum Hall plateau transitions, *Phys. Rev. B* **99**, 024205 (2019).
- [19] Q. Niu, D. J. Thouless, and Y.-S. Wu, Quantized Hall conductance as a topological invariant, *Phys. Rev. B* **31**, 3372 (1985).
- [20] A. Sterdyniak, N. Regnault, and B. A. Bernevig, Extracting Excitations from Model State Entanglement, *Phys. Rev. Lett.* **106**, 100405 (2011).
- [21] Y. J. Chung, D. Graf, L. Engel, K. V. Rosales, P. Madathil, K. Baldwin, K. West, L. Pfeiffer, and M. Shayegan, Correlated States of 2D Electrons near the Landau Level Filling $\nu = 1/7$, *Phys. Rev. Lett.* **128**, 026802 (2022).

Supplemental Material for “Impurity-induced thermal crossover in fractional Chern insulators”

Ke Huang,¹ Sankar Das Sarma,^{2,3} and Xiao Li^{1,*}

¹*Department of Physics, City University of Hong Kong, Kowloon, Hong Kong SAR, China*

²*Condensed Matter Theory Center and Joint Quantum Institute,
University of Maryland, College Park, Maryland 20742, USA*

³*Kavli Institute for Theoretical Physics, University of California, Santa Barbara, California 93106, USA*

(Dated: September 27, 2024)

In this Supplementary Material, we present our calculation of the toy model in Eq. (1) of the main text in a larger system that contains 6×4 unit cells. Compared with the $N_x \times N_y = 6 \times 3$ system in the main text, the $N_x \times N_y = 6 \times 4$ system has a dimension of 346 104 and no symmetries because of the impurities. Consequently, one cannot access the whole spectrum of the system through exact diagonalization. Nonetheless, one can still obtain hundreds of the lowest eigenvalues and eigenstates using the Lanczos algorithm. In Fig. S1, we calculate the finite-temperature density matrix using the lowest 1000 eigenstates, and the numerical density matrix is given by

$$\rho = \frac{\sum_{i=1}^{1000} e^{-e_i/T} |\psi_i\rangle\langle\psi_i|}{\sum_{i=1}^{1000} e^{-e_i/T}}, \quad (\text{S1})$$

where e_i and $|\psi_i\rangle$ are the eigenvalue and its corresponding eigenstate. In this larger system, we observe qualitatively similar phenomena to the smaller system in the main text. For $V_{\text{imp}} < 0.1$, the system manifests a crossover from Fermi liquid (FL) to fraction Chern insulator (FCI) at finite temperatures, signified by the FL entanglement gap at a lower temperature and the FCI entanglement gap at a higher temperature. Further, the temperature scale where the crossover happens T_e increases with increasing V_{imp} and eventually exceeds the FCI temperature scale T_{FCI} around $V_{\text{imp}} = 0.1$. Hence, there is not an obvious crossover to FCI for $V_{\text{imp}} > 0.1$, as shown in Fig. S1(b).

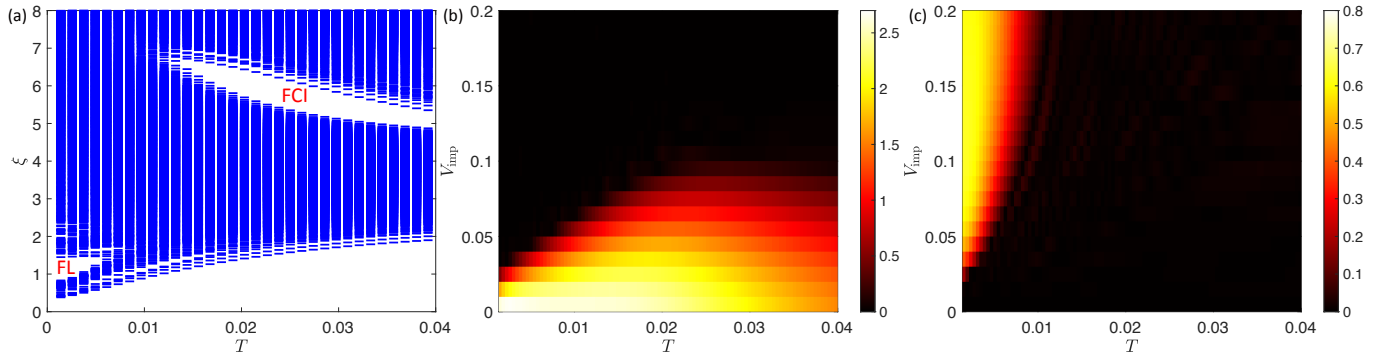


FIG. S1. (a) The particle-entanglement spectrum (PES) as a function of temperature at $V_{\text{imp}} = 0.07$. For the entanglement gap at $T \lesssim 0.01$, there are 35 states below the gap, in agreement with the quasihole excitation of FL. For the entanglement gap at $T \gtrsim 0.01$, there are 1088 states below the gap, in agreement with the (1,3)-permissible quasihole excitation of FCI. (b) Phase diagram of the entanglement gap for FCI. (c) Phase diagram of the entanglement gap for FL. Here, the system size is $N_x \times N_y = 6 \times 4$, the particle number is $n_e = 7$, the number of the impurities is $N_{\text{imp}} = 3$, and the PES is obtained by tracing out four particles.

* xiao.li@cityu.edu.hk